Myocytic androgen receptor controls the strength but not the mass of limb muscles

Céline Chambon[a], Delphine Duteil[a], Alban Vignaud[b,c], Arnaud Ferry[b,c], Nadia Messaddeq[a], Rocco Malivindi[a,d], Shigeaki Kato[e], Pierre Chambon[a,1], and Daniel Metzger[a,1]

[a]Institut de Génétique et de Biologie Moléculaire et Cellulaire, Centre National de la Recherche Scientifique Unité Mixte de Recherche 7104, Institut National de la Santé et de la Recherche Médicale U964, Université de Strasbourg, Collège de France, 67404 Illkirch, France; [b]Institut National de la Santé et de la Recherche Médicale U974, Centre National de la Recherche Scientifique Unité Mixte de Recherche 7215, Université Pierre et Marie Curie-Paris 6, 75013 Paris, France; [c]Université Paris Descartes, 75006 Paris, France; [d]Department of Pharmaco-Biology, University of Calabria, 87030 Arcavacata di Rende, Italy; and [e]Institute of Molecular and Cellular Biosciences, University of Tokyo, 113-0032 Tokyo, Japan

Contributed by Pierre Chambon, July 2, 2010 (sent for review January 29, 2010)

The anabolic effects of androgens on skeletal muscles are thought to be mediated predominantly through the androgen receptor (AR), a member of the ligand-dependent nuclear receptor superfamily. However, despite numerous studies performed in men and in rodents, these effects remain poorly understood. To characterize androgen signaling in skeletal muscles, we generated mice in which the AR is selectively ablated in myofibers. We show that myocytic AR controls androgen-induced insulin-like growth factor IEa (IGF-IEa) expression in the highly androgen-sensitive perineal muscles and that it mediates androgen-stimulated postnatal hypertrophy of these muscles. In contrast, androgen-dependent postnatal hypertrophy of limb muscle fibers is independent of myocytic AR. Thus, androgens control perineal and limb muscle mass in male mice through myocytic AR-dependent and -independent pathways, respectively. Importantly, we also show that AR deficiency in limb myocytes impairs myofibrillar organization of sarcomeres and decreases muscle strength, thus demonstrating that myocytic AR controls key pathways required for maximum force production. These distinct androgen signaling pathways in perineal and limb muscles may allow the design of screens to identify selective androgen modulators of muscle strength.

androgens | insulin-like growth factor | perineal muscles | sarcopenia | mouse

Loss of muscle mass and function is a feature of various diseases (e.g., neuromuscular disorders, cancer, sepsis, and AIDS), immobilization following acute injuries, and aging that greatly impairs the quality of life for affected patients. Clinical studies indicate that testosterone replacement in young and old hypogonadal men (1–9), as well as in men with sarcopenia associated with chronic illness (10, 11), increases skeletal muscle mass and strength. However, other clinical studies indicate that androgens stimulate muscle mass but not strength (12–14). Moreover, despite the use of androgenic steroids by athletes, the effects of these agents on athletic performance and physical functions remain poorly characterized (15).

In rodents, perineal skeletal muscles [bulbocavernosus (BC) and levator ani (LA), collectively BC/LA] are highly androgen sensitive (16). Indeed, postnatal gonadal testosterone production in males increases BC/LA muscle fiber number and muscle fiber hypertrophy at puberty (17, 18). At adulthood BC/LA fiber size decreases markedly after castration and increases with androgen treatment (19–22), but fiber number remains unchanged (23). In contrast, androgen effects on limb muscle mass and function in animal models remain controversial. Indeed, studies in mice indicate that androgen withdrawal by castration reduces fast-twitch hindlimb muscle mass and maximum force production (24, 25), whereas testosterone administration to orchidectomized male mice prevents hindlimb skeletal muscle atrophy and enhances fatigue resistance of soleus muscle (26). However, it also was reported that administration of the testosterone derivative stanozolol to mice does not increase muscle mass, force, or resistance to fatigue (27).

Androgens mediate their effects predominantly through the androgen receptor (AR), a member of the ligand-dependent nuclear receptor superfamily (28). Two natural steroids, testosterone and dihydrotestosterone, bind and activate AR to regulate target gene expression. Because AR is expressed in various cell types of skeletal muscle in mammals (e.g., fibroblasts, satellite cells, and myofibers) (29–31), as well as in motoneurons (31), all these cells are potential sites of androgen action. In addition, androgens might act through poorly characterized nongenomic pathways (32) or after aromatization by activation of estrogen receptors (33).

To characterize androgen signaling in skeletal muscle and to identify cellular target(s) through which androgens exert their effects, we generated and analyzed mice in which AR is ablated selectively and efficiently in myofibers. We show that myocytic AR transduces androgen-dependent postnatal fiber hypertrophy in perineal but not in limb skeletal muscles. In addition, we demonstrate that myocytic AR is essential to generate maximum force of fast- and intermediary-twitch leg muscles by controlling myofibrillar organization of androgen-induced hypertrophic myofibers.

Results

Generation of Mice Lacking AR Selectively in Postmitotic Skeletal Muscle Myocytes. To investigate androgen signaling in skeletal muscle, we established mice in which the AR is ablated selectively in skeletal muscle myofibers. To this end, $AR^{L2/y}$ mice bearing floxed AR L2 alleles (in which LoxP sites flank chromosome X exon 1 encoding the AR N-terminal domain) (34) were bred with HSA-Cre mice that express Cre recombinase in skeletal muscle myofibers (35–37) to produce HSA-Cre/$AR^{L2/y}$ somatic mutant male mice (hereafter called $AR^{skm-/y}$) as well as $AR^{L2/y}$ control littermates.

AR transcript levels were decreased selectively in skeletal muscles of 6-wk-old $AR^{skm-/y}$ mice (Fig. S1A). At age 15 wk, AR transcript levels were more than 5-fold lower in the fast-twitch [e.g., extensor digitorum longus (EDL) and quadriceps], mixed (e.g., gastrocnemius, tibialis), and slow-twitch (e.g., soleus) hindlimb skeletal muscles and were 3-fold lower in the BC/LA in $AR^{skm-/y}$ mice than in $AR^{L2/y}$ mice (Fig. S1B). Moreover, AR protein levels were strongly decreased in skeletal muscles of $AR^{skm-/y}$ mice (Fig. S1C). The low levels remaining probably were present in skeletal muscle fibroblasts and/or satellite cells where AR was not ablated.

MEDICAL SCIENCES

Perineal Myocytic AR Mediates Androgen-Dependent Postnatal Fiber Hypertrophy of BC/LA. Because the postnatal development of the BC/LA muscles and their maintenance in adulthood are highly androgen dependent (16), we first analyzed the effect of AR ablation in myocytes of these muscles. At 6 wk of age, the mass of the BC/LA was 2-fold lower in AR$^{skm-/y}$ mice than in AR$^{L2/y}$ mice (Fig. 1A), indicating a growth defect. Moreover, whereas the mass of BC/LA increased by 2-fold in AR$^{L2/y}$ between 6 and 13 wk of age, it was almost unchanged in AR$^{skm-/y}$ mice during this time period (Fig. 1A). At age 13 wk, the size of BC/LA was strongly reduced in AR$^{skm-/y}$ mice (Fig. 1B, *Upper*), and histological analyses showed that BC muscle fibers were smaller in AR$^{skm-/y}$ mice than in AR$^{L2/y}$ mice (Fig. 1B, *Lower*). The distribution of cross-sectional areas (CSA) of BC fibers in AR$^{L2/y}$ mice centered around 1,000–1,500 μm², whereas in AR$^{skm-/y}$ mice it was shifted to around 500–1,000 μm² (Fig. S2A), and the mean BC fiber CSA was decreased by nearly 50% in AR$^{skm-/y}$ mice (Fig. 1C). Collectively these results show that myocytic AR controls hypertrophy of perineal muscle fiber during postnatal development.

To demonstrate that myocytic AR also controls the maintenance of BC/LA muscle fiber size, we generated mice in which AR was selectively ablated in skeletal muscle myofibers at adulthood. To this end, AR$^{L2/L2}$ female mice were bred with HSA-Cre-ER^{T2} transgenic mice that express the tamoxifen-dependent Cre-ER^{T2} recombinase selectively in postmitotic skeletal muscle myocytes (38). I.p. injection of tamoxifen in 7-wk-old HSA-Cre-ER^{T2}/AR$^{L2/y}$ male mice induced efficient ablation of AR in their skeletal muscles (Fig. S3), thus generating AR$^{(i)skm-/y}$ mice. Similarly treated AR$^{L2/y}$ male littermates were used as controls. One week after the first tamoxifen administration, BC/LA weight was 20% lower in AR$^{(i)skm-/y}$ mice than in control mice (Fig. 1D) and was reduced by 25% in 25-wk-old AR$^{(i)skm-/y}$ mice (Fig. 1E). Interestingly, BC/LA mass of AR$^{L2/y}$ mice 1 mo after orchidectomy was similar to that of age-matched AR$^{skm-/y}$ mice (57.6 ± 5.1 mg vs. 62.3 ± 3.5 mg) (Fig. 1F), thus showing that myocytic AR transduces androgen signaling to maintain BC/LA fiber size in adulthood. Taken together, these results demonstrate that myocytic AR transduces BC/LA fiber hypertrophy during postnatal development and maintenance of muscle fiber size at adulthood.

Androgens have been shown to stimulate local production of insulin-like growth factor I (IGF-I) to increase muscle mass (39), and two IGF-I splice variants encoding the mechano growth factor (MGF) and IGF-IEa are expressed in rodent skeletal muscles (40). Because the regulation of MGF and IGF-IEa by androgens and their contribution to muscle hypertrophy were unknown, we compared their transcript levels in AR$^{L2/y}$ and AR$^{skm-/y}$ mice. Transcript levels of MGF were similar in BC/LA muscles of 13-wk-old control and mutant mice (Fig. S4A); IGF-IEa transcript levels were 2-fold lower in AR$^{skm-/y}$ mice than in AR$^{L2/y}$ mice (Fig. 1G), but plasma IGF-I levels were similar in AR$^{L2/y}$ and AR$^{skm-/y}$ mice (Fig. S4B). These data demonstrate that myocytic AR transduces the anabolic effects of androgens on BC/LA muscles and indicate that these effects are mediated, at least in part, by local IGF-IEa production.

Lack of AR in Skeletal Muscle Myofibers Does Not Affect Limb Muscle Mass But Impairs Strength of Fast- and Intermediary-Twitch Muscles. Weight gain was similar in AR$^{skm-/y}$ and AR$^{L2/y}$ mice over the course of more than 1 y (Fig. S5A), and the mass of various hindlimb skeletal muscles (EDL, quadriceps, gastrocnemius, tibialis, and soleus) was similar in AR$^{skm-/y}$ and AR$^{L2/y}$ mice at 6, 13, and 40 wk of age (Table 1 and Fig. 2A). Gastrocnemius and soleus muscles of AR$^{L2/y}$ and AR$^{skm-/y}$ mice had a similar gross morphology, and their histological analyses did not reveal any differences (Fig. 2B). Gastrocnemius, tibialis, and soleus fiber distribution, as well as their mean CSA, were similar in AR$^{skm-/y}$ and AR$^{L2/y}$ mice (Fig. 2C and Fig. S2 B–F). Moreover, selective ablation of AR in skeletal muscle myofibers of adult mice did not affect limb muscle mass (Fig. 2D). Taken together, these results demonstrate that myocytic AR is dispensable for postnatal leg muscle growth and maintenance of leg muscle mass in adulthood.

Because the mass of fast-twitch skeletal muscles is reduced when androgen levels are low (26), as well as in AR-null mice (41), we determined the effect of androgen deficiency in mice lacking AR selectively in skeletal muscles. One month after orchidectomy of 5-mo-old mice, the mass of fast-twitch (EDL and quadriceps) and intermediary-twitch (gastrocnemius and tibialis) skeletal muscles was similarly decreased in AR$^{L2/y}$ and AR$^{skm-/y}$ mice (Table S1 and Fig. 2E), and in both cases mean fiber CSA of gastrocnemius muscle was 20% lower than in sham-operated mice (Fig. 2F). Thus, androgen depletion leads to atrophy of fast- and intermediary-twitch muscle, irrespective of the presence of AR in myocytes. IGF-IEa transcript levels were decreased by 2-fold in gastrocnemius of AR$^{L2/y}$ after orchidectomy, indicating that decreased muscle fiber size might be a consequence of reduced IGF-IEa levels (Fig. 2G). Because a similar decrease in IGF-IEa transcript levels was observed in the gastrocnemius of orchidectomized AR$^{skm-/y}$ mice, myocytic AR does not control IGF-IEa transcript levels in limb skeletal muscles (Fig. 2G). Note that MGF transcript levels were similar in the gastrocnemius of sham-operated and orchidectomized mice of each genotype (Fig. S6). In contrast, soleus muscle mass was not affected by orchidectomy in either AR$^{L2/y}$ or AR$^{skm-/y}$ mice (Table S1). Taken together, these results show that androgens control fast- and intermediary-twitch hindlimb muscle mass through myocytic AR-independent pathways, most probably via local IGF-IEa production.

To determine whether myocytic AR controls leg skeletal muscle strength, we subjected AR$^{L2/y}$ and AR$^{skm-/y}$ mice to grip tests at various ages (Fig. 3A). Between 6 and 8 wk, maximal grip
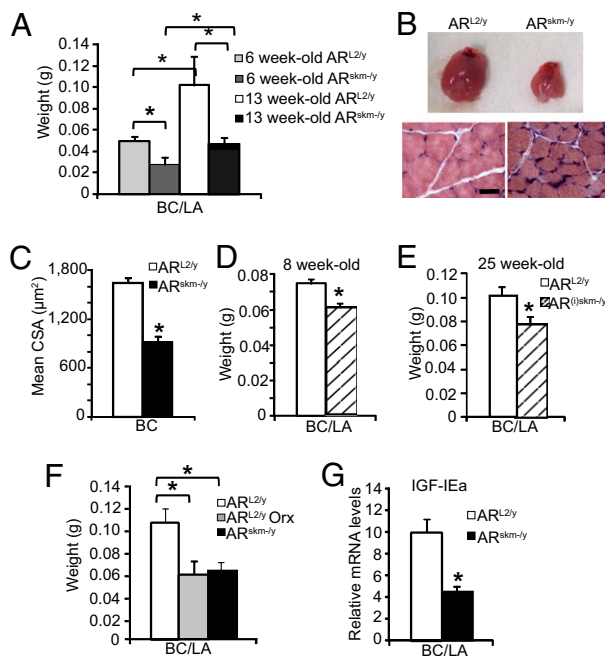

Fig. 1. Characterization of BC/LA muscles in AR$^{skm-/y}$ and AR$^{(i)skm-/y}$ mice. (*A*) BC/LA weight from 6- and 13-wk-old AR$^{L2/y}$ and AR$^{skm-/y}$ mice ($n = 7$). (*B*) Gross morphology of BC/LA (*Upper*) and histological analysis of H&E-stained BC muscle (*Lower*) of 13-wk-old AR$^{L2/y}$ and AR$^{skm-/y}$ mice. (Scale bar, 20 μm.) (*C*) Mean fiber CSA of BC muscle from 13-wk-old AR$^{L2/y}$ and AR$^{skm-/y}$ mice. (*D* and *E*) BC/LA weight from 8-wk-old (*D*) and 25-wk-old (*E*) AR$^{L2/y}$ and AR$^{(i)skm-/y}$ mice ($n = 7$). (*F*) BC/LA weight from 25-wk-old sham-operated (sham) and orchidectomized (Orx) AR$^{L2/y}$ mice, and from 25-wk-old AR$^{skm-/y}$ mice ($n = 7$). (*G*) IGF-IEa mRNA levels from 13-wk-old AR$^{L2/y}$ and AR$^{skm-/y}$ mice ($n = 8$). In *A* and *C*–*G*, error bars indicate SEM; *, $P < 0.05$.

Chambon et al.

Table 1. Hindlimb skeletal muscle mass (mg) of 6-, 13-, and 40-wk-old AR$^{L2/y}$ and AR$^{skm-/y}$ mice

Muscle	6 Wk		13 Wk		40 Wk	
	AR$^{L2/y}$	AR$^{skm-/y}$	AR$^{L2/y}$	AR$^{skm-/y}$	AR$^{L2/y}$	AR$^{skm-/y}$
EDL	16.8 ± 1.0	16.1 ± 1.3*	15.2 ± 0.9	14.8 ± 0.6*	16.7 ± 1.5	16.1 ± 1.3*
Quadriceps	140 ± 3.4	136 ± 5.9*	183.3 ± 1.2	189.9 ± 1.2*	222.6 ± 3.4	223.7 ± 7.0*
Gastrocnemius	107.6 ± 3.4	100 ± 5.9*	145.7 ± 10.0	155.8 ± 7.6*	174 ± 6.0	185.0 ± 10.0*s
Tibialis	46.2 ± 4.0	41.2 ± 4.6*	62.1 ± 3.5	62.0 ± 3.1*	68.8 ± 3.3	69.3 ± 2.1*
Soleus	9.7 ± 1.5	8.1 ± 1.0*	8.8 ± 0.7	8.3 ± 0.7*	8.6 ± 1.4	9.0 ± 1.8*

Data are expressed ± SEM; n = 7 animals per group.
*Not statistically different from AR$^{L2/y}$ mice ($P > 0.05$).

strength increased by 15% in AR$^{L2/y}$ mice and increased further to reach peak level at around 6 mo of age. With increased aging, maximal grip strength decreased progressively, and at 10 mo it was similar to the prepuberty level (Fig. 3A). In contrast, maximal grip strength of AR$^{skm-/y}$ mice did not increase at puberty,

despite increased muscle mass, and remained constant over more than 14 months (Fig. 3A and Table 1). Interestingly, ablation of AR in skeletal muscle myocytes by tamoxifen treatment of HSA-Cre-ER^{T2}/AR$^{L2/y}$ mice at 7 wk also resulted in decreased muscle strength (Fig. S7A). These results indicate that
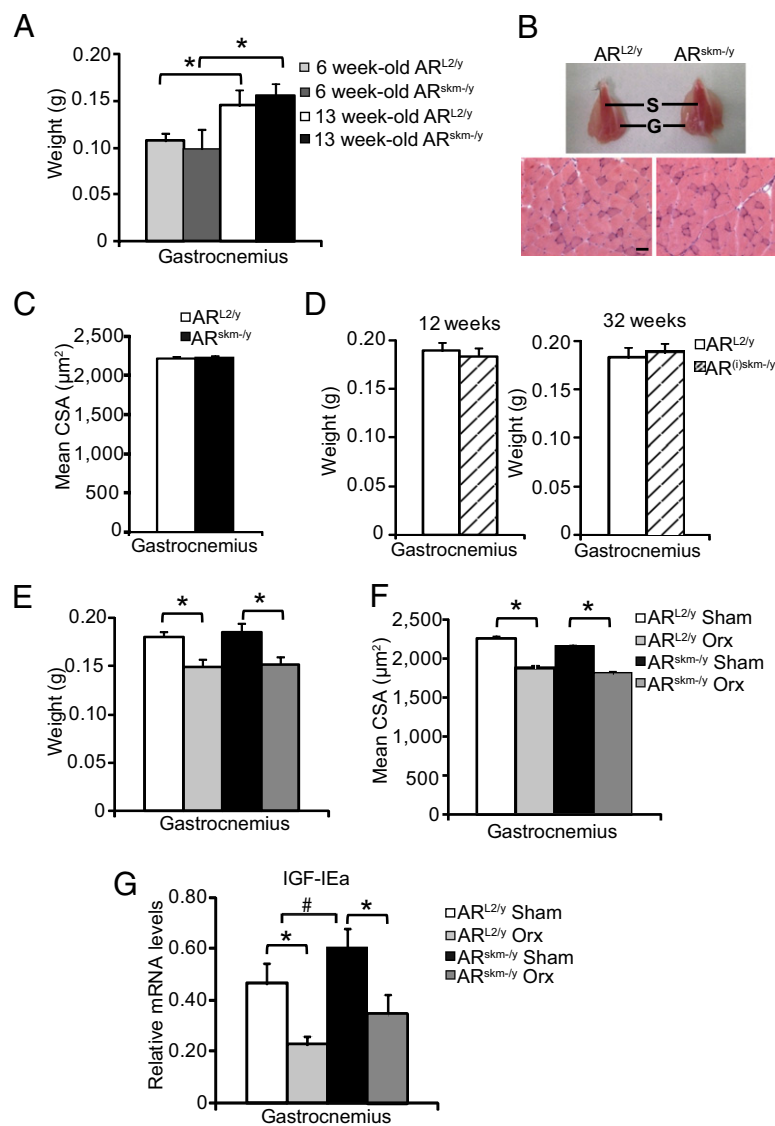

Fig. 2. Characterization of hindlimb skeletal muscles in AR$^{skm-/y}$ mice and AR$^{(i)skm-/y}$ mice. (A) Gastrocnemius weight from 6- and 13-wk-old AR$^{L2/y}$ and AR$^{skm-/y}$ mice (n = 7). (B) Gross morphology of gastrocnemius (G) and soleus (S) muscles (*Upper*) and histological analysis of H&E-stained gastrocnemius muscle (*Lower*) from 13-wk-old AR$^{L2/y}$ and AR$^{skm-/y}$ mice. (Scale bar, 20 μm.) (C) Mean fiber CSA of gastrocnemius muscle from 13-wk-old AR$^{L2/y}$ and AR$^{skm-/y}$ mice. (D) Gastrocnemius weight from 12- and 32-wk-old AR$^{L2/y}$ and AR$^{(i)skm-/y}$ mice (n = 7). Gastrocnemius weight (E), mean fiber CSA (F), and IGF-IEa mRNA levels (G) from 25-wk-old sham-operated (sham) and orchidectomized (Orx) AR$^{L2/y}$ and AR$^{skm-/y}$ mice (n = 6). In A and C–G, error bars indicate SEM. In A, F, and G, *P < 0.05. In G, #P ≥ 0.05.
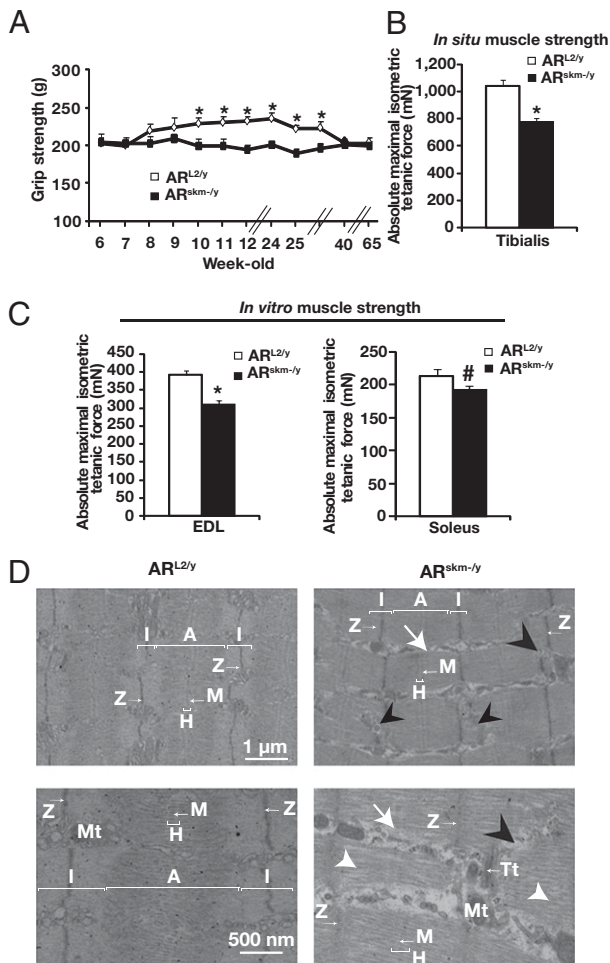
Chambon et al.

MEDICAL SCIENCES

www.manaraa.com

Fig. 3. Characterization of muscle contractile functions in AR[skm-/y] mice. (A) Maximal grip strength of AR[L2/y] and AR[skm-/y] mice between the ages of 6 and 65 wk (n = 8–10). (B) In situ absolute maximal isometric tetanic force of tibialis anterior muscle from 20-wk-old AR[L2/y] and AR[skm-/y] mice (n = 7–8). (C) In vitro absolute maximal isometric tetanic force of EDL and of soleus muscles from 20-wk-old AR[L2/y] and AR[skm-/y] mice (n = 7–8). In A–C, error bars indicate SEM; *$P < 0.05$. In C, #$P = 0.84$. (D) Ultrastructure of EDL muscle from 15-wk-old AR[L2/y] and AR[skm-/y] mice. Black arrowheads indicate Z line disruptions; white arrowheads indicate loss of myofilaments; white arrows indicate sarcoplasm. A, A band; I, I band; H. H band; M, M line; Mt, mitochondria; Tt, T-tubules; Z, Z line.

myocytic AR is critically involved in specific maximal force production of limb muscles.

To characterize further limb muscles lacking AR selectively in myocytes, in situ tibialis anterior contractile properties were analyzed in 20-wk-old mice. Maximal tetanic force and maximal tetanic force relative to muscle weight in response to nerve stimulation were 25% lower in AR[skm-/y] mice than in AR[L2/y] littermates (Fig. 3B and Fig. S5B). To determine whether this decrease was caused by neuromuscular defects or alterations of intrinsic contractile functions, muscle force was determined in vitro. Maximal tetanic force and specific tetanic force in response to muscle stimulation was 20% lower in the fast-twitch EDL of AR[skm-/y] mice than of AR[L2/y] mice but was unchanged in the slow-twitch soleus muscle (Fig. 3C and Fig. S5C). Fatigue resistance was similar in intermediary- and fast-twitch skeletal muscles of AR[skm-/y] and AR[L2/y] mice and was slightly reduced in the slow-twitch soleus muscle of AR[skm-/y], without reaching statistical significance (Fig. S5D). Collectively, these results demonstrate that

myocytic AR controls intrinsic contractile functions of fast- and intermediary-twitch hindlimb skeletal muscles.

Lack of AR in Myocytes Induces Myofibrillar Disruption. To investigate whether the impaired specific strength of muscles in AR[skm-/y] mice was a consequence of alterations in the contractile apparatus, we performed ultrastructural analyses. Electron microscopy of EDL, tibialis and gastrocnemius from 15-wk-old AR[skm-/y] mice revealed disruptions of myofibrils in about 10% of the sarcomeres from AR[skm-/y] mice, with loss of myofilaments, rupture of Z lines, and enlarged sarcoplasm (Fig. 3D and Fig. S8 A and B). These myofibrillar alterations were distributed randomly in skeletal muscle sarcomeres. Despite these defects, no sign of fiber degeneration, inflammation, or atrophy was observed in skeletal muscles of AR[skm-/y] mice. In contrast, no myofibrillar disruption was observed in slow-twitch skeletal muscles (e.g., soleus) of mutant mice (Fig. S8C). It is noteworthy that the defects exhibited in gastrocnemius muscle of AR[(i)skm-/y] mice were similar to those of AR[skm-/y] mice (Fig. S7B). Taken together, these data demonstrate that myocytic AR is essential for proper myofibril organization of fast- and intermediary-twitch skeletal muscles.

Discussion

We have shown here, in agreement with a recent report (42), that selective ablation of AR in skeletal muscle myofibers results in a reduction of perineal muscle fiber size and mass. Moreover, because either castration or selective AR ablation in myofibers at adulthood decreases perineal muscle mass similarly, myocytic AR transduces androgen-dependent BC/LA muscle hypertrophy (Fig. 4). In contrast, mass and fiber size of limb skeletal muscles were similar in adult AR[skm-/y] and control mice, demonstrating that myocytic AR does not control postnatal growth of these skeletal muscles. Because castration induced a similar reduction in leg muscle mass in AR[skm-/y] and control mice, androgens mediate leg muscle hypertrophy in a myocytic AR-independent pathway. Thus, androgen anabolic effects in leg muscles might be transduced by other cellular targets (e.g., satellite cells) (Fig. 4). Differential responses in perineal and leg muscles might result from a higher number of AR-expressing myonuclei in perineal than in limb muscles (29) or from cell-specific transcriptional activities of AR in these muscles.

Our results also demonstrate that androgens differentially regulate IGF-I transcript variants in skeletal muscles of adult mice. Indeed, whereas IGF-IEa transcript levels were androgen dependent in both perineal and leg skeletal muscles, MGF transcript levels were androgen independent. Interestingly, IGF-IEa expression was dependent on myocytic AR in BC/LA muscles but not in leg skeletal muscles (Fig. 4). Because IGF-IEa has been shown to stimulate protein synthesis in skeletal muscle to increase muscle fiber size (40), it is likely that androgen-stimulated muscle fiber hypertrophy in adult mice is mediated, at least in part, by IGF-IEa produced by satellite cells or myofibroblasts.

Importantly, even though selective AR ablation in skeletal muscle myofibers induced by Cre recombinase expressed under the control of the human skeletal actin promoter did not affect leg muscle mass, the strength of fast- and intermediary-twitch muscles was reduced selectively because of alterations in myofibrillar organization in some of their sarcomeres (Fig. 4). Similar defects were induced by AR ablation in skeletal muscle myofibers in adulthood, thus demonstrating that myocytic AR controls pathways required for maximum force production. Whether myocytic AR regulates the expression and/or turnover of myofibrillar cytoskeletal proteins remains to be determined.

Our data are in sharp contrast with those of Ophoff et al. (42). Indeed, their study, based on analyses of mARKO mutant mice in which AR was ablated selectively in postmitotic myocytes using
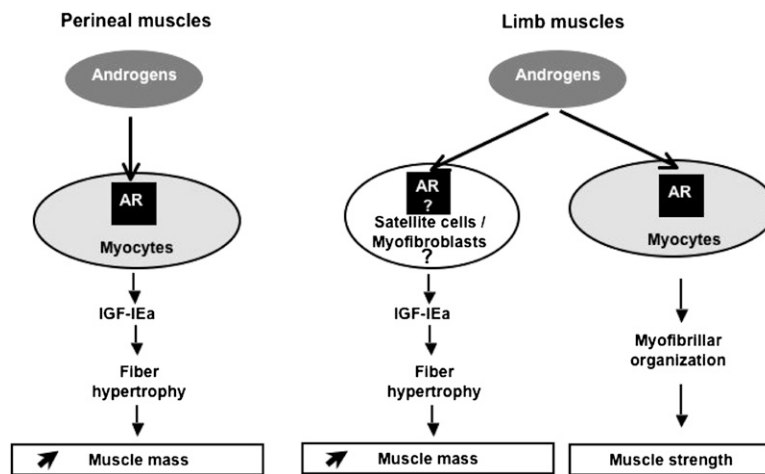
Perineal muscles

Limb muscles

Fig. 4. Schematic model of androgen signaling in perineal and limb skeletal muscles.

MCK-Cre transgenic mice, showed that the EDL muscle mass was decreased but did not reveal any defect in intrinsic muscle strength (42). The results also are unexpected from previous studies of mice in which AR is ablated in the germ line, because decreased EDL strength in these mutant mice was attributed to decreased muscle mass, and no intrinsic contractile dysfunctions could be detected (41, 42). Note, however, that MacLean et al. (41) reported a decreased mass of slow-, intermediary-, and fast-twitch muscle in AR-null mice and an increased resistance to fatigue in slow-twitch muscles, whereas Ophoff et al. (42) observed decreased mass in fast- but not slow-twitch muscles and no impairment in fatigue resistance in the soleus muscle. The reasons for these discrepancies are unknown.

In summary, our results highlight the complexity of androgen signaling pathways in skeletal muscle. Our data show that androgens induce muscle fiber hypertrophy through different pathways in perineal and leg skeletal muscles (Fig. 4). Importantly, we also demonstrate that AR ablation in skeletal muscle myocytes impairs intrinsic contractile functions in fast- and intermediary-twitch muscle. Thus, even though perineal muscles are very sensitive to androgen anabolic effects, their use is not appropriate to identify selective AR modulators that may stimulate muscle strength in peripheral skeletal muscles. Our study opens avenues to identify selective AR modulators that (i) stimulate muscle strength without increasing the risk of cardiovascular and liver diseases, as well as prostate cancer, associated with testosterone therapy, and (ii) inhibit the progression of prostate cancer without inducing skeletal muscle weakness.

Methods

Mice. Mice were maintained in a temperature- and humidity-controlled animal facility with a 12-h light/dark cycle and free access to water and a standard rodent chow (2,800 kcal/kg Usine d'Alimentation Rationelle). Body weight was determined at various ages. Animals were killed at the beginning of the light cycle by CO_2 inhalation, and tissues were collected, weighed, and frozen in liquid nitrogen or processed for biochemical and histological analysis. Breeding and maintenance of mice were performed under institutional guidelines, and all experimental protocols were approved by the Animal Care and Use Committee of the Institut de Génétique et de Biologie Moléculaire et Cellulaire.

Generation of AR$^{skm-/y}$ and AR$^{(i)skm-/y}$ Mice. HSA-Cre (35) and HSA-Cre-ER^{T2} mice (38) were described previously. AR L2 alleles were generated by Cre-mediated excision of the neomycin resistance gene in ES cells bearing AR L3 alleles (34). AR$^{skm-/y}$ mice were generated by breeding mice carrying "floxed" AR L2 alleles with HSA-Cre transgenic mice. To generate AR$^{(i)skm-/y}$ mice, mice carrying "floxed" AR L2 alleles were bred with HSA-Cre-ER^{T2} transgenic mice, and HSA-Cre-ER^{T2}/AR$^{L2/y}$ male mice, bearing the HSA-Cre-ER^{T2} transgene and

AR L2 alleles, were tamoxifen-treated daily for 5 d at age 7 wk, as described (43). Tamoxifen-treated AR$^{L2/y}$ and oil (vehicle)-treated and HSA-Cre-ER^{T2}/AR$^{L2/y}$ male littermates were used as controls.

Grip Strength. A grip strength meter (Bioseb) was used to measure forelimb and hindlimb grip strength. The test was repeated three consecutive times within the same session, and the mean value was recorded as the maximal grip strength for each mouse.

Contractile Measurements. In situ isometric tibialis anterior muscle force in response to nerve stimulation was performed as described previously (44), and muscle masses were measured to calculate specific maximal force. Fatigue resistance was assessed after repeated contractions (75 Hz for 500 ms, evoked once every second for 100 s), and the time to reach half the initial force was calculated (FR). Measurements of in vitro isometric contractile properties of soleus and EDL muscles were performed according to previously described methods (45). Specific maximal tetanic force (mN/mm^5) was calculated by dividing the force by the estimated cross-sectional area of the muscle. Assuming muscles have a cylindrical shape and a density of 1.06 mg mm^{-3}, the muscle cross-sectional area corresponds to the wet weight of the muscle divided by its fiber length (L_f). L_f to L_0 ratio of 0.7 (soleus) or 0.45 (EDL) was used to calculate L_f. L_0 is the fiber length at which maximal tetanic force is observed. Fatigue resistance was assessed by repeated isometric tetanic (75 Hz for 300 ms, evoked once every second for 200 s), and FR was calculated. All data provided by the muscle lever were recorded and analyzed on a microcomputer, using the PowerLab/4SP system (AD Instruments).

Orchidectomy. AR$^{L2/y}$ and AR$^{skm-/y}$ mice were sham operated or orchidectomized at age 21 wk and were killed 1 mo later.

IGF-I Plasma Levels. Plasma IGF-I levels were measured at Institut Clinique de la Souris, using mouse IGF-I Quantikine ELISA kit (R&D Systems) (46).

Histological Analysis. Muscles were quickly frozen in dry ice-cooled isopentane. For H&E staining, 10-μm cryosections were stained with Harris hematoxylin (VWR International S.A.S.), washed in running tap water, decolorized in acid alcohol for 2 s, stained in eosin (VWR International S.A.S.), washed in running tap water, dehydrated, cleared, and mounted. For muscle fiber CSA, all surface fibers of a muscle section were determined using MetaMorph software (Molecular Devices).

Electron Microscopy Skeletal muscle samples were fixed by immersion in 2.5% glutaraldehyde and 2.5% paraformaldehyde in cacodylate buffer (0.1 M, pH 7.4), washed in cacodylate buffer for 30 min, and kept at 4 °C. Postfixation was performed with 1% osmium tetroxide in 0.1 M cacodylate buffer for 1 h at 4 °C, and dehydration was performed with graded alcohol (50, 70, 90, and 100%) and propylene oxide for 30 min each. Samples were oriented longitudinally and embedded in Epon 812 (Sigma Chimie). Ultrathin sections were cut at 70 nm, contrasted with uranyl acetate and lead citrate, and examined at 70 kV

Chambon et al.

www.manaraa.com

with a Morgagni 268D electron microscope. Images were captured digitally by a Mega View III camera (Soft Imaging System).

RNA Preparation and Analysis. RNA was isolated using TRIzol Reagent (Invitrogen). We converted 5 μg RNA to cDNA with SuperScript II reverse transcriptase (Invitrogen Life Technologies) and hexamers primers according to the supplier's protocol. Quantitative RT-PCR was performed by using the QuantiTectTM SYBR Green PCR kit (Qiagen) according to the supplier's protocol. Hypoxanthine-guanine phosphoribosyltransferase (HPRT) was used as an internal control. Primers were as follows:

HPRT 5′-GTTGGATACAGGCCAGACTTTGTTG-3′, 5′- GATTCAACTTGCGCTC-ATCTTAGGC-3′; AR 5′-CTGCCTCCGAAGTGTGGTAT-3′, 5′-GCCAGAAGCTTCAT-CTCCAC-3′; MGF 5′-AGCTGCAAAGGAGAAGGAAAGGAAG-3′, 5′-GGTGATGTG-GCATTTCCTGCT-3′; IGF-IEa 5′-TGACATGCCCAAGACTCA- 3′, 5′ -TGTGGCATTT-TCTGCTCCGTGG -3′.

Protein Preparation and Analysis. Proteins were isolated using RIPA buffer [50 mM Tris (pH 7.5), 1% Nonident p40, 0.5% sodium deoxycholate, 0.1% SDS, 150 mM NaCl, 5 mM EDTA, 1 mM PMSF, and containing a mixture of protease inhibitors (45 μg/mL)]. Homogenates (50 μg of protein) were electrophoresed in 8% acrylamide gels. Proteins were electroblotted to Hybond nitrocellulose membranes (Amersham Biosciences), and proteins of interest were immuno-detected using primary antibodies directed against AR (N-20, 1/200; Santa Cruz) (42) and GAPDH (1/50,000; Millipore/Upstate/Chemicon). Secondary antibodies (1/10,000) conjugated to HRP (Jackson ImmunoResearch) were detected using an enhanced chemiluminescence detection system (Thermo Scientific).

Data Analysis. Data are presented as mean ± SEM. Differences analyzed by a two-tailed Student's t test were considered statistically significant at $P < 0.05$ and are indicated in the figures by an asterisk.

1. Bhasin S, et al. (1997) Testosterone replacement increases fat-free mass and muscle size in hypogonadal men. *J Clin Endocrinol Metab* 82:407–413.
2. Katznelson L, et al. (1996) Increase in bone density and lean body mass during testosterone administration in men with acquired hypogonadism. *J Clin Endocrinol Metab* 81:4358–4365.
3. Brodsky IG, Balagopal P, Nair KS (1996) Effects of testosterone replacement on muscle mass and muscle protein synthesis in hypogonadal men—a clinical research center study. *J Clin Endocrinol Metab* 81:3469–3475.
4. Wang C, et al. (1996) Sublingual testosterone replacement improves muscle mass and strength, decreases bone resorption, and increases bone formation markers in hypogonadal men—a clinical research center study. *J Clin Endocrinol Metab* 81:3654–3662.
5. Wang C, et al., Testosterone Gel Study Group (2000) Transdermal testosterone gel improves sexual function, mood, muscle strength, and body composition parameters in hypogonadal men. *J Clin Endocrinol Metab* 85:2839–2853.
6. Morley JE, et al. (1993) Effects of testosterone replacement therapy in old hypogonadal males: A preliminary study. *J Am Geriatr Soc* 41:149–152.
7. Sih R, et al. (1997) Testosterone replacement in older hypogonadal men: A 12-month randomized controlled trial. *J Clin Endocrinol Metab* 82:1661–1667.
8. Urban RJ, et al. (1995) Testosterone administration to elderly men increases skeletal muscle strength and protein synthesis. *Am J Physiol* 269:E820–E826.
9. Tenover JL (2000) Experience with testosterone replacement in the elderly. *Mayo Clinic Proc* 75 Suppl:S77–81.
10. Bhasin S, et al. (2000) Testosterone replacement and resistance exercise in HIV-infected men with weight loss and low testosterone levels. *JAMA* 283:763–770.
11. Reid IR, Wattie DJ, Evans MC, Stapleton JP (1996) Testosterone therapy in glucocorticoid-treated men. *Arch Intern Med* 156:1173–1177.
12. Tenover JS (1992) Effects of testosterone supplementation in the aging male. *J Clin Endocrinol Metab* 75:1092–1098.
13. Snyder PJ, et al. (1999) Effect of testosterone treatment on body composition and muscle strength in men over 65 years of age. *J Clin Endocrinol Metab* 84:2647–2653.
14. Snyder PJ, et al. (2000) Effects of testosterone replacement in hypogonadal men. *J Clin Endocrinol Metab* 85:2670–2677.
15. Wilson JD (1988) Androgen abuse by athletes. *Endocr Rev* 9:181–199.
16. Sengelaub DR, Forger NG (2008) The spinal nucleus of the bulbocavernosus: Firsts in androgen-dependent neural sex differences. *Horm Behav* 53:596–612.
17. Tobin C, Joubert Y (1991) Testosterone-induced development of the rat levator ani muscle. *Dev Biol* 146:131–138.
18. Joubert Y, Tobin C (1995) Testosterone treatment results in quiescent satellite cells being activated and recruited into cell cycle in rat levator ani muscle. *Dev Biol* 169:286–294.
19. Wainman P, Shipounoff GC (1941) The effects of castration and testosterone propionate on the striated perineal musculature in the rat. *Endocrinology* 29:975–978.
20. Dorfman RD, Kincl FA (1963) Relative potency of various steroids in an anabolic androgenic assay using castrated rat. *Endocrinology* 72:259–266.
21. Vyskocil F, Gutmann E (1977) Anabolic effect of testosterone on the levator ani muscle of the rat. *Pflugers Arch* 371:3–8.
22. Balice-Gordon RJ, Breedlove SM, Bernstein S, Lichtman JW (1990) Neuromuscular junctions shrink and expand as muscle fiber size is manipulated: In vivo observations in the androgen-sensitive bulbocavernosus muscle of mice. *J Neurosci* 10:2660–2671.
23. Venable JH (1966) Morphology of the cells of normal, testosterone-deprived and testosterone-stimulated levator ani muscles. *Am J Anat* 119:271–301.
24. Jiang B, Klueber KM (1989) Structural and functional analysis of murine skeletal muscle after castration. *Muscle Nerve* 12:67–77.
25. Rowe RW (1968) Effect of castration on muscle growth in the mouse. *J Exp Zool* 169:59–64.
26. Axell AM, et al. (2006) Continuous testosterone administration prevents skeletal muscle atrophy and enhances resistance to fatigue in orchidectomized male mice. *Am J Physiol Endocrinol Metab* 291:E506–E516.
27. Tingus SJ, Carlsen RC (1993) Effect of continuous infusion of an anabolic steroid on murine skeletal muscle. *Med Sci Sports Exerc* 25:485–494.
28. MacLean HE, Warne GL, Zajac JD (1997) Localization of functional domains in the androgen receptor. *J Steroid Biochem Mol Biol* 62:233–242.
29. Johansen JA, Breedlove SM, Jordan CL (2007) Androgen receptor expression in the levator ani muscle of male mice. *J Neuroendocrinol* 19:823–826.
30. Sinha-Hikim I, Taylor WE, Gonzalez-Cadavid NF, Zheng W, Bhasin S (2004) Androgen receptor in human skeletal muscle and cultured muscle satellite cells: Up-regulation by androgen treatment. *J Clin Endocrinol Metab* 89:5245–5255.
31. Monks DA, O'Bryant EL, Jordan CL (2004) Androgen receptor immunoreactivity in skeletal muscle: Enrichment at the neuromuscular junction. *J Comp Neurol* 473:59–72.
32. Foradori CD, Weiser MJ, Handa RJ (2008) Non-genomic actions of androgens. *Front Neuroendocrinol* 29:169–181.
33. Walters KA, Allan CM, Handelsman DJ (2008) Androgen actions and the ovary. *Biol Reprod* 78:380–389.
34. Shiina H, et al. (2006) Premature ovarian failure in androgen receptor-deficient mice. *Proc Natl Acad Sci USA* 103:224–229.
35. Miniou P, et al. (1999) Gene targeting restricted to mouse striated muscle lineage. *Nucleic Acids Res* 27:e27 (i–iv).
36. Monks DA, et al. (2007) Overexpression of wild-type androgen receptor in muscle recapitulates polyglutamine disease. *Proc Natl Acad Sci USA* 104:18259–18264.
37. Nicole S, et al. (2003) Intact satellite cells lead to remarkable protection against Smn gene defect in differentiated skeletal muscle. *J Cell Biol* 161:571–582.
38. Schuler M, Ali F, Metzger E, Chambon P, Metzger D (2005) Temporally controlled targeted somatic mutagenesis in skeletal muscles of the mouse. *Genesis* 41:165–170.
39. Chen Y, Zajac JD, MacLean HE (2005) Androgen regulation of satellite cell function. *J Endocrinol* 186:21–31.
40. Goldspink G, Harridge SD (2004) Growth factors and muscle ageing. *Exp Gerontol* 39:1433–1438.
41. MacLean HE, et al. (2008) Impaired skeletal muscle development and function in male, but not female, genomic androgen receptor knockout mice. *FASEB J* 22:2676–2689.
42. Ophoff J, et al. (2009) Androgen signaling in myocytes contributes to the maintenance of muscle mass and fiber type regulation but not to muscle strength or fatigue. *Endocrinology* 150:3558–3566.
43. Schuler M, et al. (2006) PGC1alpha expression is controlled in skeletal muscles by PPARbeta, whose ablation results in fiber-type switching, obesity, and type 2 diabetes. *Cell Metab* 4:407–414.
44. Lahoute C, et al. (2008) Premature aging in skeletal muscle lacking serum response factor. *PLoS One* 3:e3910.
45. Agbulut O, et al. (2009) Slow myosin heavy chain expression in the absence of muscle activity. *Am J Physiol Cell Physiol* 296:C205–C214.
46. Entingh-Pearsall A, Kahn CR (2004) Differential roles of the insulin and insulin-like growth factor-I (IGF-I) receptors in response to insulin and IGF-I. *J Biol Chem* 279:38016–38024.

www.manaraa.com